AIMS Materials Science, 13(2): 187–204.
DOI: 10.3934/matersci.2026011
Received: 10 November 2025
Revised: 15 January 2026
Accepted: 06 February 2026
Published: 27 February 2026

https://www.aimspress.com/journal/Materials

Research article

Development and characterization of a polymer composite based on coal fly ash and expanded polystyrene waste: Toward sustainable valorization

Saleh Eladaoui[1], Mouad El Mouzahim[1,2], El Mehdi Eddarai[1,*], Mustapha El Kanzaoui[1], Abdelkbir Bellaouchou[1] and Ratiba Boussen[1]

[1] Laboratory of Materials, Nanotechnology, and Environment, Mohammed V University in Rabat, Faculty of Sciences, Av. Ibn Battouta, Agdal-Rabat, BP 1014, Morocco
[2] Department of Chemistry, Life Sciences and Environmental Sustainability, University of Parma, INSTM, UdR Parma, Parco Area delle Scienze 17/A, Parma, 43124, Italy

* **Correspondence:** Email: elmehdi.eddarai@gmail.com.

Abstract: In the context of developing sustainable materials and promoting environmental protection through the valorization of solid wastes, a thermoplastic composite was fabricated using coal fly ash (FA) and expanded polystyrene (EPS) waste. FA was employed as the reinforcing filler, while EPS waste, dissolved in acetone, served as the polymer matrix. Composites were prepared by incorporating varying weight fractions of FA, ranging from 20 to 80 wt.%, into the polystyrene matrix via compression molding. The resulting materials were thoroughly characterized to evaluate their mineralogical, physicochemical, mechanical, and microstructural properties. The findings indicated that an optimal composite composition containing 70 wt.% fly ash and 30 wt.% polystyrene matrix exhibited a compressive strength up to 15 MPa. In this study, we not only present a novel composite material but also address environmental concerns by contributing to the reduction of solid and plastic waste pollution.

Keywords: coal fly ash; expanded polystyrene waste; valorization; fly ash-polystyrene composite; waste management

1. Introduction

The development of sustainable materials that meet key requirements such as high strength, low weight, and durability has attracted considerable attention. Polymer matrix composites have shown great potential to fulfill these demands [1]. Plastic waste generated in large quantities, such as polystyrene, offers an alternative source of raw material for the development of polymer matrix composites. Polystyrene alone accounts for approximately 10 wt.% of the total plastic waste produced worldwide, representing nearly 15 million tons annually [2,3]. Polystyrene is a hydrocarbon thermoplastic polymer with a very low density (20 to 30 kg/m^3), which contains 98% air and only 2% polystyrene; it is mostly used for thermal insulation, packaging, and storing of many products due to its flexible structure, impact absorption property, impermeability, and mechanical robustness; in addition, polystyrene has a stable form in the presence of many chemicals and does not perform chemical reactions except some kinds of acids, solvents, and aliphatic compounds that dissolve it [4–6]. It is challenging to collect expanded polystyrene due to its low bulk density. Reducing the volume of polystyrene remains one of the best approaches to collect it. Chemical and thermal techniques are generally adapted to reduce the volume of polystyrene and thus make their recycling easy [7]. Thus, researchers have carried out studies on the use of polystyrene based matrix (polystyrene dissolved in solvent) as a matrix in the elaboration of composite materials; several raw materials, organic and inorganic, have been used as fillers for polystyrene composites [8–10]. Masri et al., [11] involved the use of date palm leaflets as the reinforcement into polystyrene matrix. The researchers found that date palm leaflets-polystyrene composite are 50% more insulating than similar composites based on wood waste and polystyrene found in the literature, and their mechanical properties are suitable and can be improved through the preparation process. Adeniyi et al. [12] explored the elaboration of hybrid composites by the reinforcement of polystyrene matrix with kaolin clay and expanded polyethylene powder and investigated their microstructural and mechanical properties. The authors showed that the incorporation of kaolin clay enhance the mechanical proprieties. However, they emphasized that the study is important for its role in converting multiple types of solid waste into valuable products. This approach not only addresses waste management but also creates useful engineering materials from recycled materials.

Moreover, solid wastes generated from industrial production activity remain one of the most solicited renewable resources that can be employed as reinforcements in polymer composite materials [13,14]. Coal fly ash (FA) generated from coal combustion in thermal power plants is one of those industrial by-products [15]. Around the world, the amount of FA generated annually by thermal power plants is approximately 750 million tons per year [16]. The amount of generated FA is increasing as thermal power plants increase. FA is mainly composed of silica (SiO_2), alumina, iron oxide, lime, and magnesia. Physicochemical and mineralogical properties of FA depend on the type of coal used in thermal power plants, combustion conditions, how the fumes are treated, and the nature of storage [17].

The use of coal FA as a filler in polystyrene-based matrix (polystyrene dissolved in solvent) to develop polymer composites at ambient temperature is unreported. Within this framework, we aim to develop a new composite material based on coal fly ash and polystyrene wastes. FA was used as the reinforcing material and polystyrene, dissolved in acetone, as the matrix. This work not only suggests the elaboration of a new composite material but also leads to reducing the pollution associated with disposal solid and plastic wastes.

2. Materials and methods

2.1. Principal materials

FA used in this study was obtained from the Supercritical Power Plant of Safi, Morocco, and it was used without modifications. The FA was collected from the electrostatic separator after the combustion of ground coal in a pulverized boiler at a temperature of more than 1400 °C. FA is an alum inosilicate material in the form of a dark grey powder, soft to the touch, similar to cement, as shown in Figure 1. The X-ray diffraction (XRD) analysis result for FA material shows that it is mostly composed of quartz (SiO_2) and mullite ($3Al_2O_3{\cdot}2SiO_2$), as verified by many researchers [18,19]. Additionally, we note the presence of an amorphous aluminosilicate phase (indicated by the broad hump between 20 and 30°) (Figure 2) [20]. Moreover, the microscopic morphology of FA, presented in Figure 1, was analyzed using scanning electron microscope (SEM). It is shown that FA particles are mainly spherical crystallized glass beads, and their surfaces are smooth and dense (area 1). In addition, FA consists of discrete amorphous ash particles with irregular shapes that are mainly generated by rapid cooling and combustion temperature (area 2) [21]. Polystyrene (PS) was collected from the plastic wastes management stock of the Faculty of Sciences Rabat, Morocco.

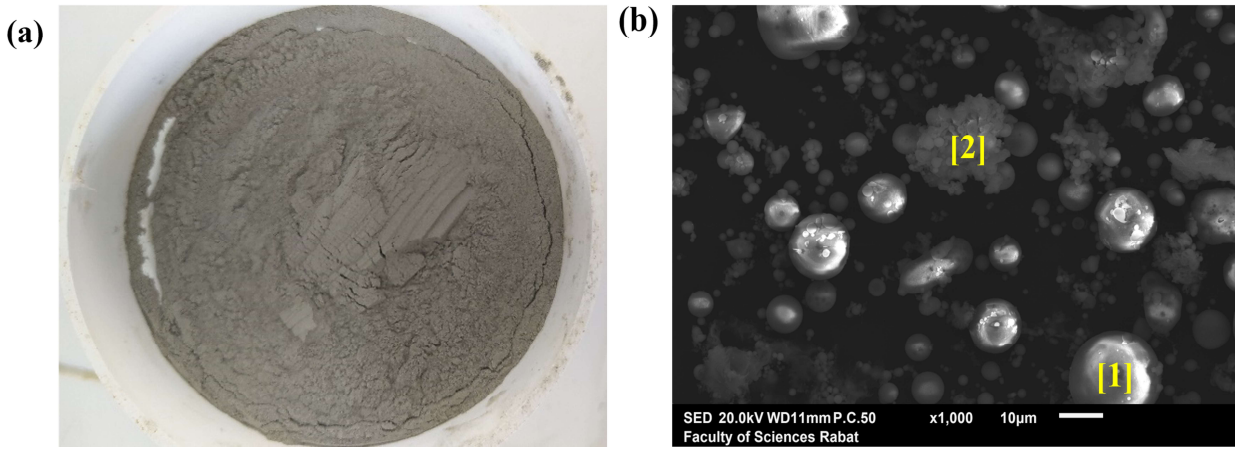

Figure 1. (a) Macroscopic and (b) microscopic aspects of coal fly ash particles.

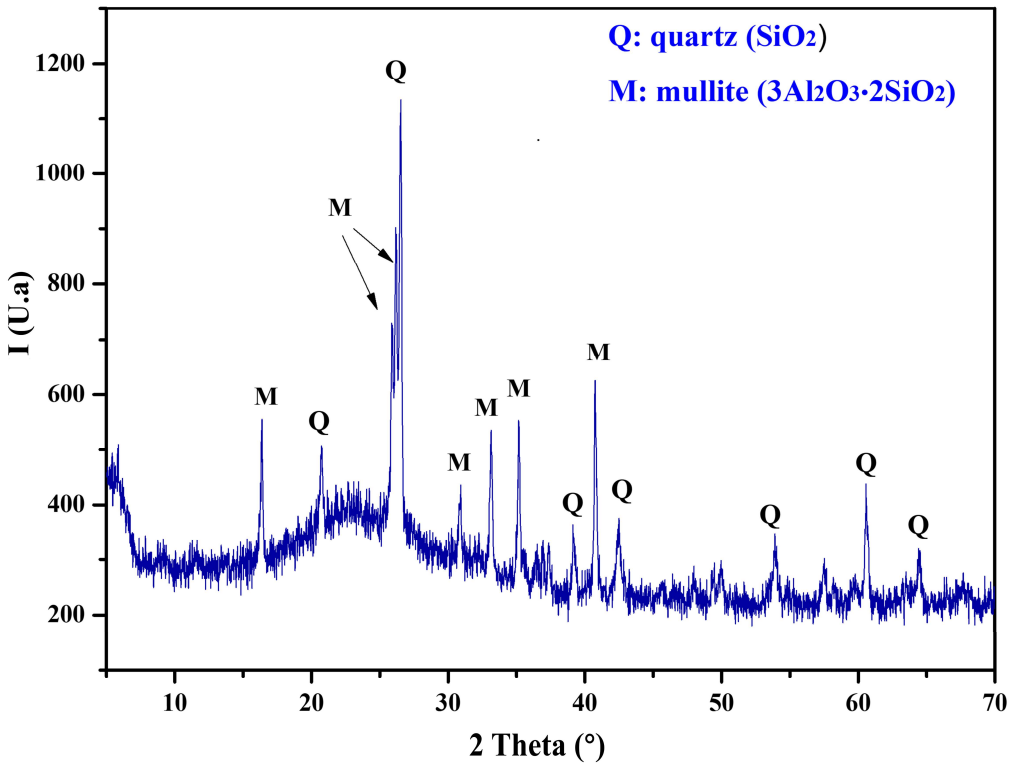

Figure 2. Mineralogical composition of fly ash from XRD patterns.

2.2. Preparation of polystyrene matrix

The polystyrene matrix used for the fabrication of FA–PS composites was obtained by dissolving expanded polystyrene waste (Figure 3a) in acetone (784 kg/m^3), according to the mass ratio defined in Eq 1; the prepared matrix is presented in Figure 3b.

$$\frac{M_{PS}}{M_{ac}} = 0.56 \tag{1}$$

Where M_{PS} is the mass of polystyrene waste and M_{ac} is the mass of acetone.

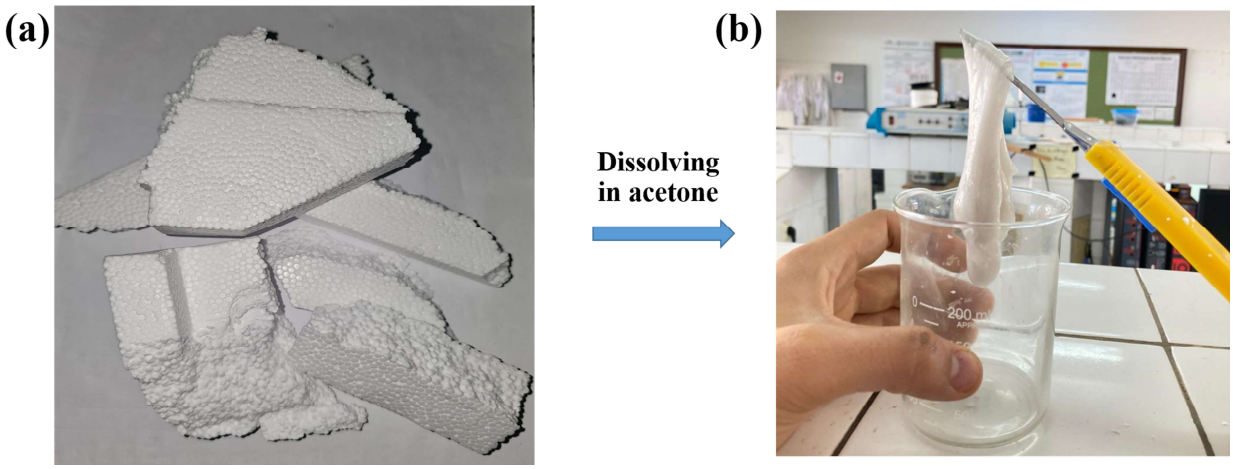

Figure 3. (a) Expanded polystyrene and (b) polystyrene matrix.

2.3. Preparation of the FA-PS composites

FA and PS were the major components used in this study as two types of solid waste materials mixed at various ratios. FA-PS composites were obtained by mixing the resulting polystyrene paste, used as the thermoplastic matrix, and the reinforcement by incorporating FA particles by ratios of 20%, 30%, 40%, 50%, 60%, 70%, and 80% (Table 1). Each mixture of FA particles and recycled PS were mixed manually to ensure total homogenization between the two wastes. The mixtures were compressed in a steel cylindrical mold to produce the final composites under a pressure of 250 MPa for at least 2 min. The resulting FA-PS composites were stored at room temperature for 28 days to complete reaction and solidification before analyzing and testing.

Table 1. Mixture proportions of FA-PS composites (wt.%).

Composite samples	Fly ash (wt.%)	Polystyrene matrix (wt.%)
FA80-PS20	80	20
FA70-PS30	70	30
FA60-PS40	60	40
FA50-PS50	50	50
FA40-PS60	40	60
FA30-PS70	30	70
FA20-PS80	20	80

2.4. Characterization of the FA-PS composites

2.4.1. Water absorption and apparent density

Water absorption and apparent density of FA-PS samples were performed based on Archimedes principle, according to ASTM, 2006. The water absorption of FA-PS samples was determined according to Eq 2 [22]:

$$Water\ absorption\ (\%) = \frac{W_2 - W_1}{W_1} \quad (2)$$

where W_2 was the weight of FA-PS samples after being boiled in water for 5 h and immersed for an additional 24 h. W_1 was the weight of FA-PS samples before being immersed in water.

2.4.2. XRD analysis

XRD analysis was performed using a LabX XRD-6100 Shimadzu diffractometer with copper anode Cu-Kα radiation (λ = 1.5418 Å) in the angular range of 2θ = 10–70° with a step size of 2°/min operating at a voltage of 40 kV and an ampere rating of 30 mA.

2.4.3. Fourier Transform infrared spectroscopy (FTIR) analysis

The FTIR analysis was performed using a VERTEX 70 in the wavelength range from 400 to 4000 cm^{-1} with a spectral resolution of 4 cm^{-1}. The FTIR spectra were taken in transmittance mode.

2.4.4. Thermal analysis (TG-DTG)

A (labsys Evo 1F) SETARAM was employed for thermal analysis (TG-TDG) with linear heating from room temperature (~20 °C) to 1000 °C and at a rate of 10 °C/min under a nitrogen atmosphere.

2.4.5. SEM

The morphology of FA and FA-PS samples was analyzed using a JEOLJSM-IT-100 SEM equipped with an energy dispersive X-ray (EDX).

2.4.6. Compressive strength

The compressive strength of the synthesized FA-PS composites was measured in accordance with ASTM C1231 (2010) using cylindrical samples (2 cm in diameter and 3.6 cm in height) after 28 days of curing. Testing was performed with an RP25 ATF hydraulic press at a loading rate of 0.5 MPa/s. For each formulation, a minimum of three replicate samples were tested, and the average value was reported as the representative compressive strength.

3. Results and discussion

3.1. Macroscopic appearance

Macroscopic examination of the FA-PS composites, presented in Figure 4, revealed that samples containing less than 50% of PS deformed and lost their cylindrical shape during the curing process. In contrast, composites with PS contents above 50% retained their initial cylindrical geometry. Moreover, the hardening of the samples was influenced by the polystyrene matrix, which hardened more rapidly as the amount of FA in the composite increased. This behavior can be attributed to the ability of FA to quickly absorb acetone, which subsequently evaporates due to its high volatility [23].

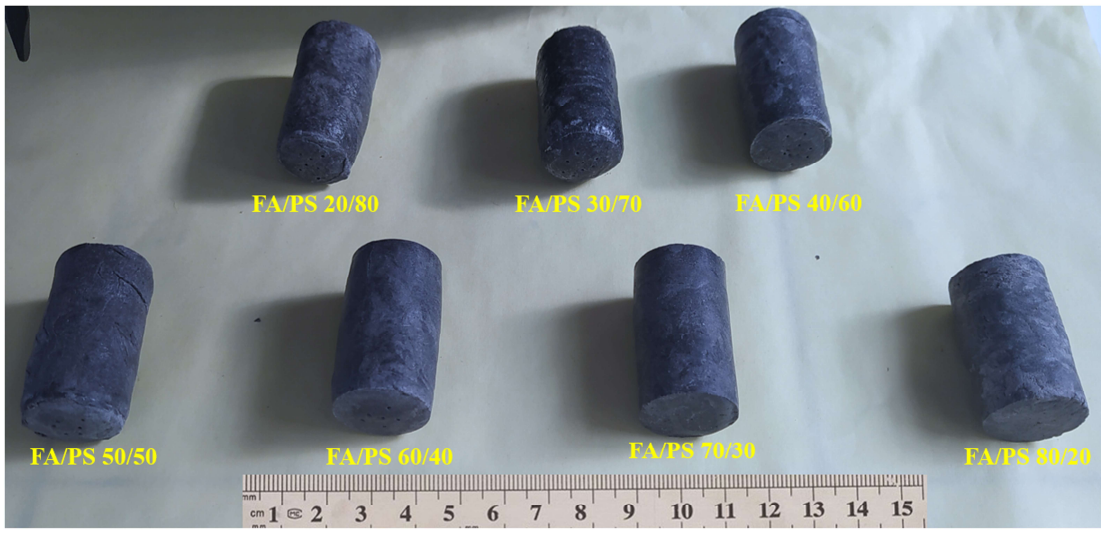

Figure 4. Macroscopic appearance of elaborated FA-PS composites with varying fly ash/polystyrene ratios (20/80 to 80/20).

3.2. Water absorption and density

Water absorption is a key indicator of the water resistance of FA-PS composites, as it provides valuable insight into their porosity and microstructural characteristics. The water absorption results for the FA-PS composites are presented in Figure 5. Overall, the results indicated that the FA-PS composites exhibited low water absorption rates. As the PS content increased from FA-PS20 to FA-PS80, the water absorption decreased significantly from 4.34% to only 0.14%. These results demonstrated that increasing the PS content reduced the water absorption of FA-PS composites. This behavior was attributed to the hydrophobic nature of PS, whose closed-cell porous structure effectively limits water penetration [24]. However, as the FA content increased, the water absorption rate also rose, indicating that FA enhances the water absorption behavior of FA-PS composites. Overall, these results showed that increasing the polystyrene matrix is essential to improve water resistance and strengthen structural integrity, while limiting degradation, which is particularly advantageous from the point of view of durability. The density results of the FA-PS composites are also presented in Figure 5, illustrating the effect of varying PS ratios on composite density. The density values decreased with increasing PS content. Specifically, the FA-PS20 composite exhibited the highest density (1.554 g/cm^3), whereas the FA-PS80 composite showed the lowest density (0.712 g/cm^3). This reduction was mainly attributed to the intrinsically low density of PS. The low-density characteristic of FA-PS composites highlights their potential for lightweight structural applications.

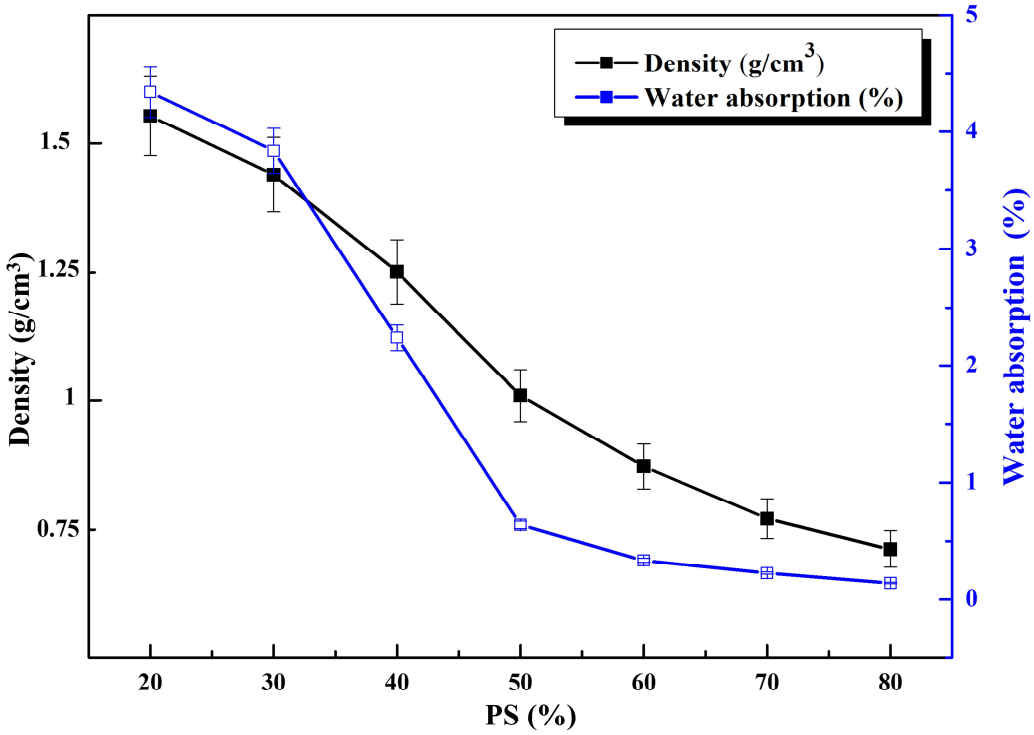

Figure 5. Density and water absorption of the produced FA-PS composites.

3.3. Thermogravimetric analysis (TGA)

The TGA was performed to investigate the weight loss versus the temperature for FA-PS composites with varying FA contents from 20 to 80 wt.%. The results of the TGA and its derivative

curves (DTG) are presented in Figure 6. Generally, all samples exhibited a similar degradation behavior characterized by a single-phase decomposition starting at 300 °C, with maximum decomposition occurring at 450 °C. Thus, the one large peak in Figure 6, which shows the derivation of the weight change of each FA-PS composite (i.e., differential TGA curve), confirmed this decomposition. Similar observations have been reported for polystyrene based composites [25,26]. This phase resulted in a weight loss ranging from 19.5 wt.% for the FA80-PS20 sample to 68 wt.% for the FA20-PS80 sample, which can be attributed to the decomposition of the cyclic structure of polystyrene matrix to volatiles styrene monomers [27]. This result incidatec that as the fly ash content increased from 20 to 80 wt.%, the total weight loss significantly decreased, indicating the presence of thermally stable phases, which enhance the thermal stability of the FA-PS composites. This improved thermal stability is attributed to the inert nature of FA contents, which originates from combustion and contains only minimal amounts of volatiles and moisture and includes non-decomposable phases such as SiO_2 and $3Al_2O_3 \cdot 2SiO_2$ [28,29]. These inorganic constituents remain thermally stable during heating, contributing to the increased residual mass at elevated temperatures, leading to enhanced overall thermal stability of the FA-PS composites.

It is also worth noting that the 5% of weight loss presented by the two composite samples FA70-PS30 and FA80-PS20 could be due to the evaporation of the residual acetone, which begins after the softening of the PS around 300 °C [30].

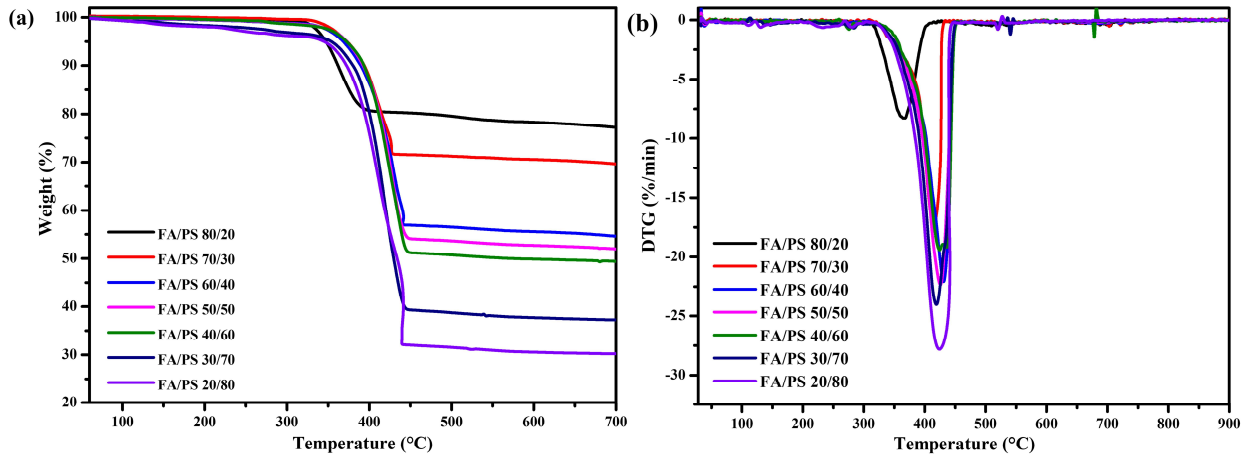

Figure 6. TGA of FA-PS composites: (a) TGA curves and (b) DTG curves.

3.4. SEM/EDS analysis

The SEM was used to investigate the microstructure of the FA-PS composites and distribution of FA particles into polystyrene matrix. Figure 7 presents the SEM micrographs of fractured surfaces FA80-PS20, FA50-PS50, and FA20-PS80 composites, respectively. In contrast to the unfilled polystyrene matrix, which exhibited a flat and smooth surface [31], the FA-PS composites displayed rough and irregular morphologies, reflecting the incorporation and distribution of FA particles. The micrographs further revealed a biphasic structure, in which the FA particles were dispersed within the polystyrene matrix. The microstructural observations revealed distinct differences among the three composite formulations. In the FA20-PS80 sample, the polystyrene matrix consituted the continuous phase, effectively embedding the FA particles and producing a relatively homogeneous microstructure

with a smooth surface and minimal void formation. However, the limited amount of FA reduced the reinforcement effect, resulting in modest mechanical performance. In the FA50-PS50 sample, a more noticeable entanglement of polymer chains around FA particles was observed, leading to the formation of larger particle aggregates. Despite this increased interaction, the interfacial bonding remained insufficient, enabling micro-voids to persist within the structure. This led to reduced structural cohesion and consequently lower compressive strength. Conversely, the FA80-PS20 sample exhibited a more compact and continuous microstructure. The higher FA content promoted closer particle packing and increased the extent of particles matrix contact. Although the amount of PS was lower, it remained sufficient to form a continuous binding phase around the ash particles, enhancing interfacial adhesion. This result correlated well with the high compressive strength recorded for this composition.

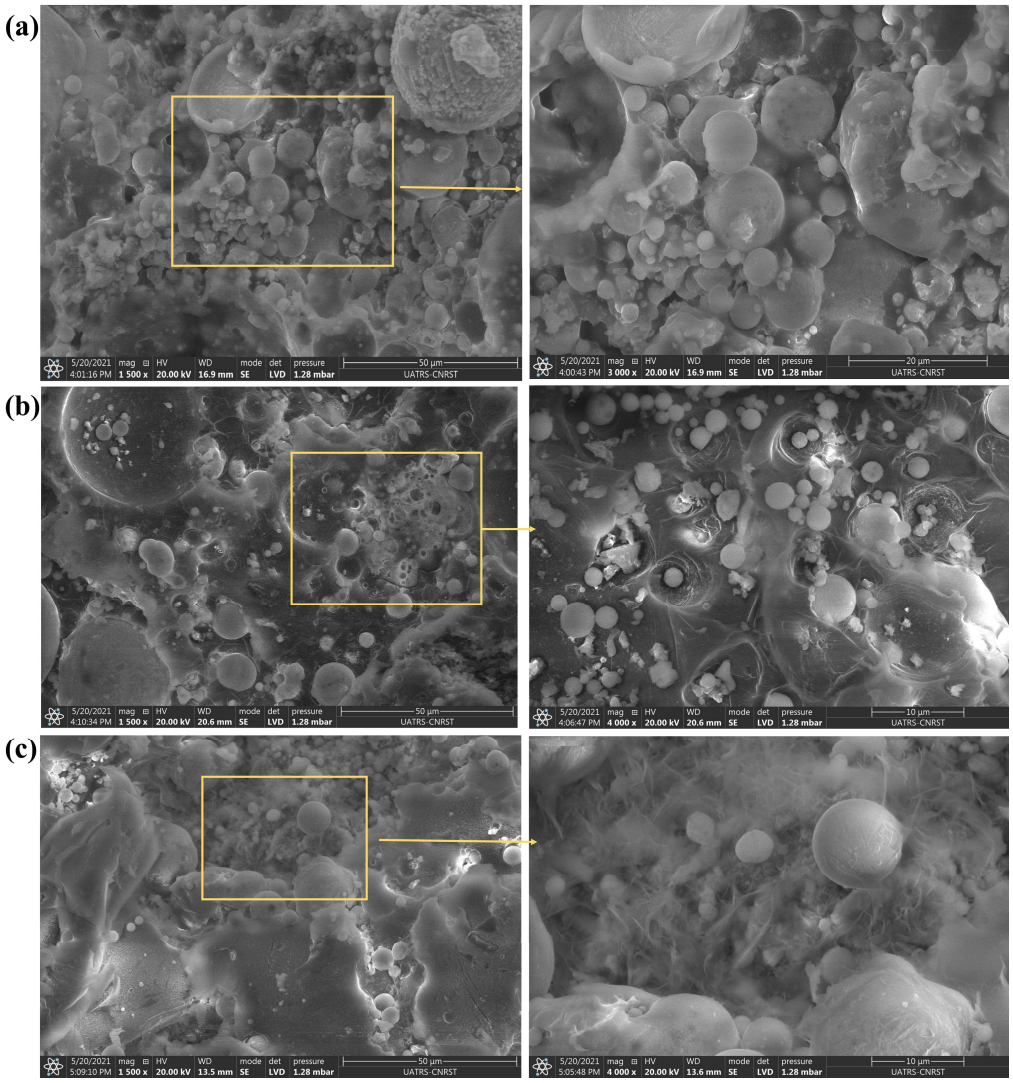

Figure 7. SEM micrographs for FA-PS composites: (a) FA80-PS20; (b) FA50-PS50; and (c) FA20-PS80.

The diagrams of the chemical composition, expressed by weight concentration and obtained at an intensity of 20 keV, are displayed in Figure 8. The results indicated that the major chemical elements present in the FA-PS composites are carbon (C), oxygen (O), silicon (Si), and aluminum (Al).

Moreover, the weight concentrations of oxygen, silicon, and aluminum increased as the FA content increased. This result agreed with XRD analysis, indicating that coal FA is mainly composed of SiO_2 and $3Al_2O_3 \cdot 2SiO_2$. However, the concentration by weight of C increased as the content of polystyrene matrix increased, reflecting its organic nature, which was consistent with the carbon-rich character of the polymer matrix, as confirmed by the EDS map showing the distribution of the principal chemical elements in the FA-PS composites illustrated in Figure 9. Additionally, the presence of other elements such as magnesium (Mg), phosphorus (P), calcium (Ca), potassium (K), iron (Fe), and titanium (Ti) was detected in the samples, and their weight concentrations increased with increasing FA content.

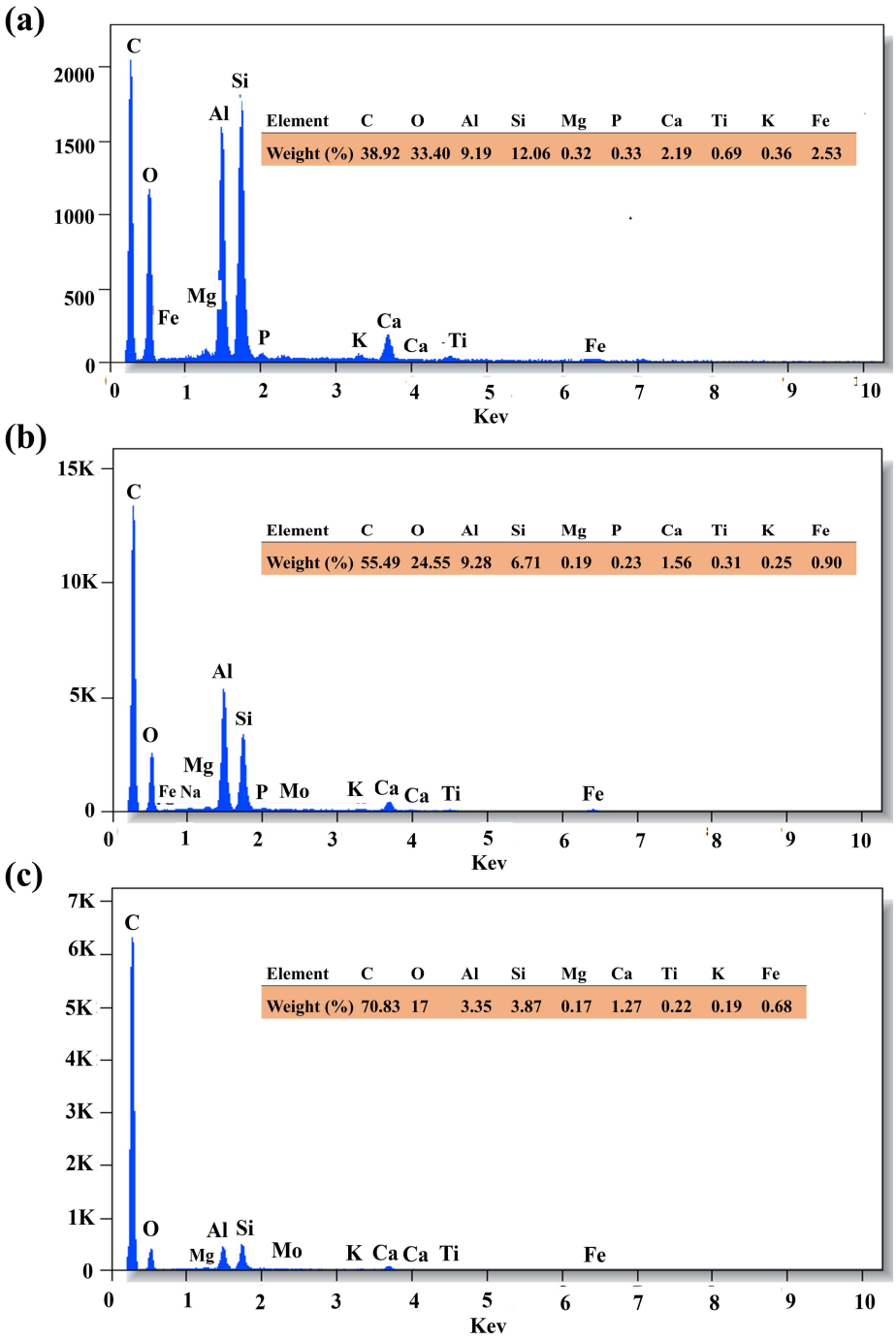

Figure 8. EDS chemical analysis of FA-PS composites: (a) FA80-PS20; (b) FA50-PS50; and (c) FA20-PS80.

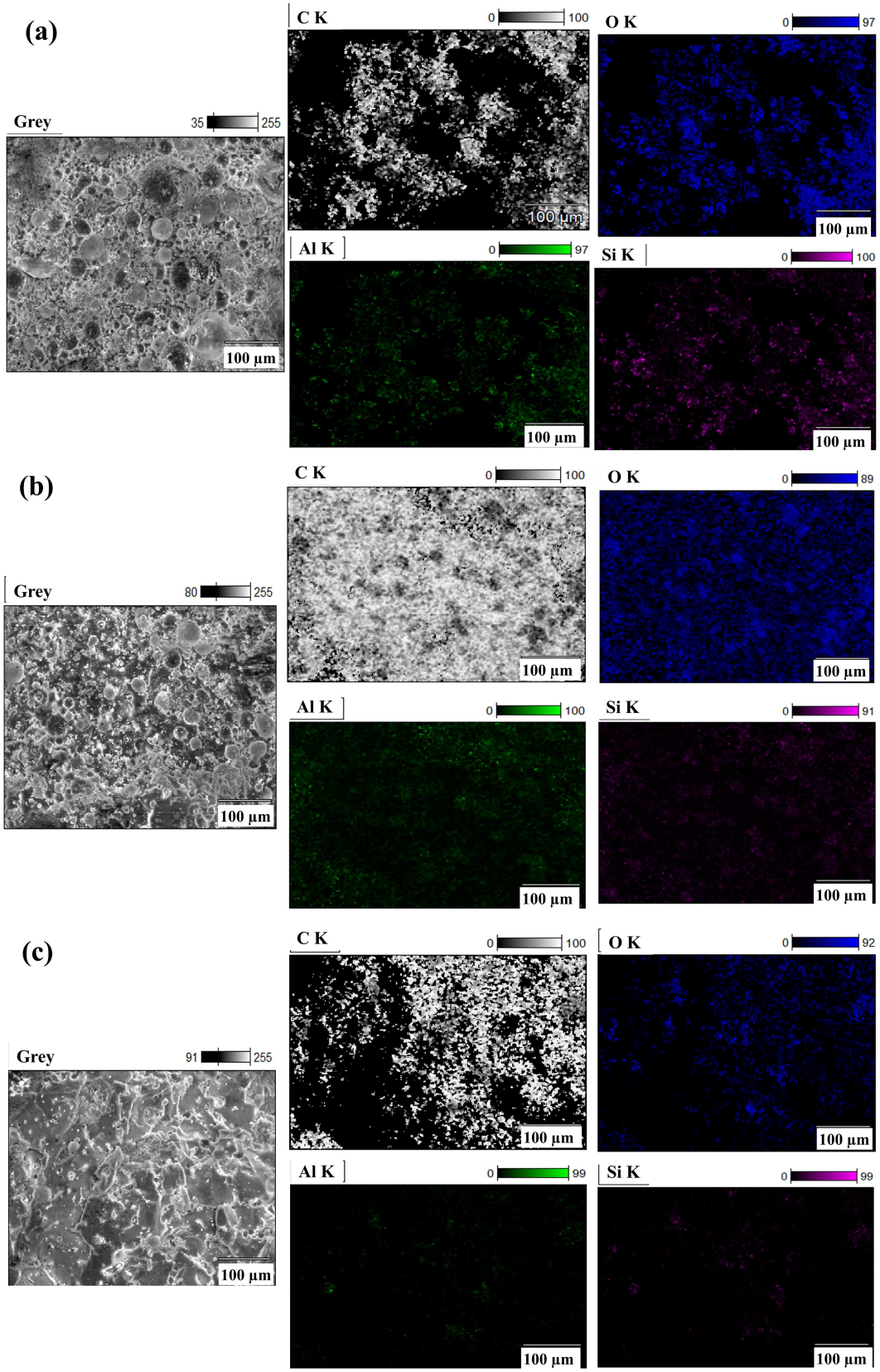

Figure 9. Combination of SEM micrographs and EDS map showing the distribution of principles chemicals elements into FA-PS composites: (a) FA80-PS20; (b) FA50-PS50; and (c) FA20-PS80.

3.5. FTIR analysis

The infrared spectroscopic was used to determine functional groups present in the FA-PS composites, the characteristic bands are listed in Table 2. The FTIR results are illustrated in Figure 10 and indicate the presence of bands related to the two major components of the manufactured composites. The band between 3060 and 3025 cm^{-1} was attributed to the aromatic stretching vibration of an alkene carbon–hydrogen bend (C–H) [32]. However, the two peaks at 2920 and 2845 cm^{-1} were also assigned to asymmetric and symmetric stretching vibration of the alkene C–H [33,34]. In addition, the peaks between 1600 and 1450 cm^{-1} were related to the C–C stretch aromatic of phenyl [35], and the two peaks at 746 and 697 cm^{-1} were attributed to a monosubstituted benzene ring [36]. The previous bands and peaks became intense in the FTIR spectra with the increase of the percentage of PS in FA-PS composites. This indicated that all previous peaks were associated with the presence of the polystyrene matrix [32–36]. Furthermore, a major absorption band appeared between 1263 and 974 cm^{-1}, and that centered in ~1072 cm^{-1} was associated with the presence of T–O (T = Al; Si) asymmetric stretching vibrations that corresponded to quartz present in FA [37]. A small band appeared at 550 cm^{-1} was attributed to symmetric stretching of Al–O–Si in mullite, which is also present in FA. However, the band associated with Si–O–Si and O–Si–O in bending vibration was at 470 cm^{-1} [38]. This result confirmed the presence of certain characteristic properties of the precursor materials (polystyrene matrix and coal fly ash) in the formulated composites. The incorporation of FA into the matrix appeared to involve chemical interactions, as evidenced by the appearance and disappearance of characteristic peaks. The emergence of new peaks suggested the formation of new chemical bonds, while the disappearance of some original peaks indicated the breaking of existing bonds during the composite formation process.

Table 2. FTIR characteristic bands.

Wavenumber (cm^{-1})	Characteristic band	References
3060	C–H aromatic stretching vibration	[32,33]
3025		
2920	C–H asymmetric stretching vibration	[33]
2845	C–H symmetric stretching vibration	[33,34]
1600–1450	Phenyl ring stretching vibration	[33,35]
1263–974 (centred in1072)	T–O asymmetric stretching vibration (T = Al, Si)	[37]
746	Mono-substituted benzene ring	[35,36]
697		
550	Symmetric stretching of Al–O–Si in mullite	[38]
470	Si–O–Si and O–Si–O in bending vibration	[38]

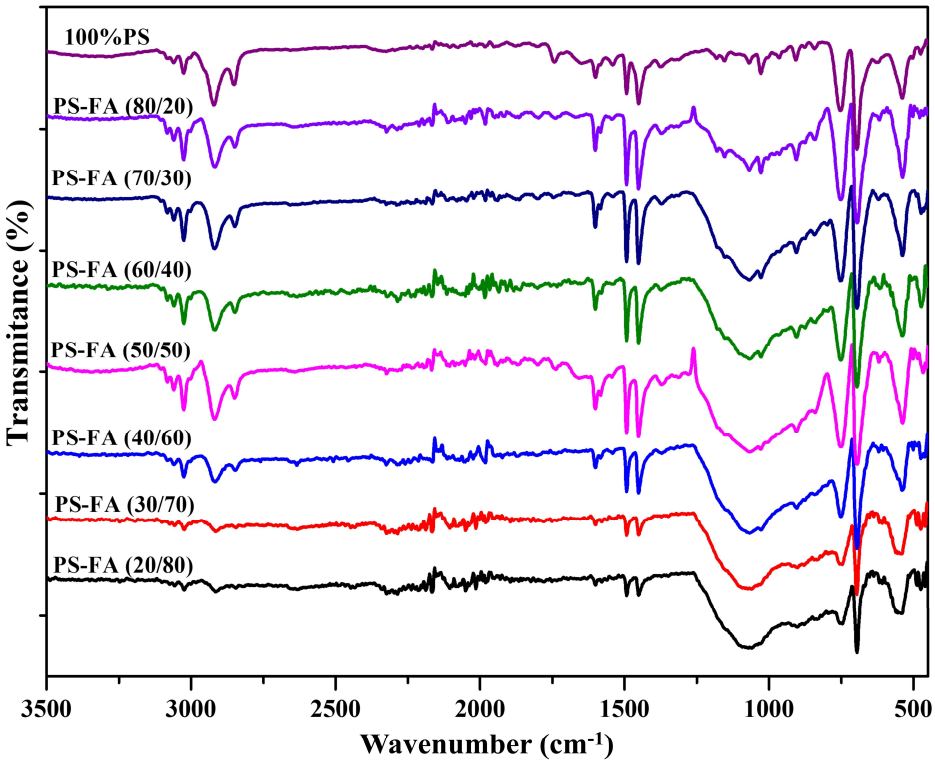

Figure 10. FTIR spectra of FA-PS composites.

3.6. Compressive strength test

The compressive strength test remains an important parameter to investigate the mechanical performance of FA-PS composites. Figure 11 shows the effect of FA content weight ratio on the compressive strength behavior of FA-PS composites at 28 days of curing. For FA-PS samples with FA contents between 30% and 60%, the compressive strength remained relatively low, ranging between 2.5 and 4.2 MPa, indicating limited contribution of FA to the mechanical performance in this range. A significant improvement was observed in the composite FA70-PS30, where the compressive strength sharply increased to approximately 15 MPa, reporting that this proportion provides an optimal cohesion between FA and polystyrene matrix. This result indicated that the increase of FA content enhances the mechanical performance of the final FA-PS composites, which is related to the reactivity of FA defined by the presence of a high amount of the amorphous aluminosilicate phase, as shown by its mineralogical composition. However, for FA80-PS20, the compressive strength decreased to 12.5 MPa, which may have been attributed to the excessive FA content causing weaker bonding as well as an insufficient polymer matrix to maintain structural integrity. Overall, the results reported an optimum FA content of 70 %, giving FA-PS composites with the highest compressive strength.

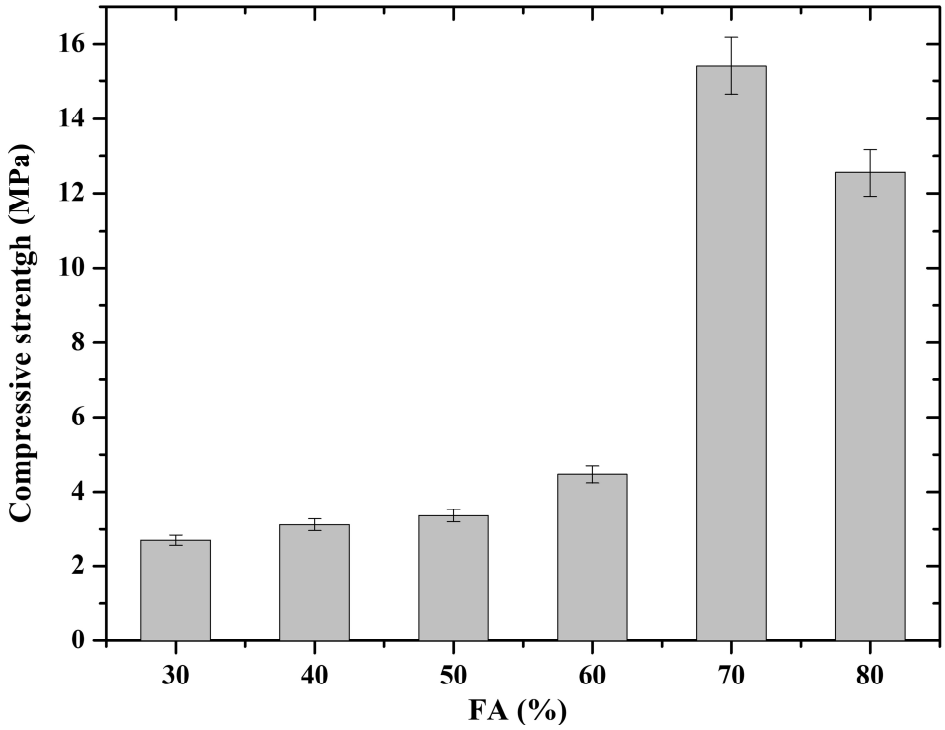

Figure 11. Compressive strength of FA-PS composites as a function of fly ash weight ratio.

4. Conclusions

In order to reduce the environmental pollution related to mineral and plastic wastes, new composite material was developed based on coal fly ash by-product and expanded polystyrene wastes. FA by-product was used as reinforcement and expanded polystyrene waste, dissolved in acetone, was used as a matrix. In this work, the mineralogical, thermal, microstructural, and mechanical properties of the composites were performed to characterize the FA-PS composites. It was observed that the presence of FA enhanced the thermal property of the composite more than the presence of the polystyrene matrix. The FTIR results suggested that a chemical reaction was taking place between the FA and the polystyrene matrix. This was reflected in the appearance of new peaks and the disappearance of others, indicating changes in the chemical structure of the material. Moreover, these chemical interactions were further supported by the EDX analysis, which showed carbon as the dominant element across all the composite samples. Furthermore, a maximum compressive strength of 15 MPa at 28 days was achieved for FA70-PS30, highlighting their potential as substitute materials in various applications. Overall, we successfully demonstrated the recycling of waste materials to create a novel composite with promising properties. In future studies, researchers should focus on optimizing the fabrication process to enhance these properties and broaden the potential applications of the material.

Use of AI tools declaration

The authors declare they have not used Artificial Intelligence (AI) tools in the creation of this article.

Acknowledgments

The first author wishes to acknowledge the Moroccan National Centre for Scientific Research (CNRST) for a scholarship grant.

Author contributions

Eladaoui Saleh: Conceptualization, methodology, investigation, data curation formal analysis, writing-original draft; El Mouzahim Mouad: Methodology, investigation, formal analysis, writing-original draft; Eddari El Mehdi: Investigation, data curation, formal analysis, writing; El Kanzaoui Mustapha: Investigation, formal analysis, writing-review & editing; Boussen Ratiba: Investigation, methodology, project administration, resources, supervision, validation, visualization, writing-original draft, writing-review & editing; Bellaouchou Abdelkbir: Supervision, writing-review & editing.

Conflict of interest

The authors declare no conflict of interest.

References

1. Hsissou R, Seghiri R, Benzekri Z, et al. (2021) Polymer composite materials: A comprehensive review. *Compos Struct* 262: 113640. https://doi.org/10.1016/j.compstruct.2021.113640
2. Aljabri NM, Lai Z, Hadjichristidis N, et al. (2017) Renewable aromatics from the degradation of polystyrene under mild conditions. *J Saudi Chem Soc* 21: 983–989. http://dx.doi.org/10.1016/j.jscs.2017.05.005
3. Kumar V, Khan A, Rabnawaz M, et al. (2022) Efficient depolymerization of polystyrene with table salt and oxidized copper. *ACS Sustainable Chem. Eng* 10: 6493–6502. https://doi.org/10.1021/acssuschemeng.1c08400
4. Koksal F, Mutluay E, Gencel O, et al. (2020) Characteristics of isolation mortars produced with expanded vermiculite and waste expanded polystyrene. *Constr Build Mater* 236: 117789. https://doi.org/10.1016/j.conbuildmat.2019.117789
5. Ferrándiz-Mas V, Bond T, García-Alcocel E, et al. (2014) Lightweight mortars containing expanded polystyrene and paper sludge ash. *Constr Build Mater* 61: 285–292. https://doi.org/10.1016/j.conbuildmat.2014.03.028
6. Fernando PLN, Jayasinghe MTR, Jayasinghe C, et al. (2017) Structural feasibility of expanded polystyrene (EPS) based lightweight concrete sandwich wall panels. *Constr Build Mater* 139: 45–51. https://doi.org/10.1016/j.conbuildmat.2017.02.027
7. Poletto M, Dettenborn J, Zeni M, et al. (2011) Characterization of composites based on expanded polystyrene wastes and wood flour. *Waste Manag* 31: 779–784. https://doi.org/10.1016/j.wasman.2010.10.027
8. Jimenez-Francisco M, Caamal-Canche JA, Carrillo JG, et al. (2018) Performance assessment of a composite material based on kraft paper and a resin formulated with expanded polystyrene waste: A case study from Mexico. *J Polym Environ* 26: 1573–1580. https://doi.org/10.1007/s10924-017-1073-7

9. Adeniyi AG, Abdulkareem SA, Adeyanju CA, et al. (2023) Mechanical and morphological analyses of flamboyant seed pod biochar/aluminium filings reinforced hybrid polystyrene composite. *J Indian Acad Wood Sci* 20: 28–36. https://doi.org/10.1007/s13196-023-00311-4
10. Adeniyi AG, Abdulkareem SA, Ighalo JO, et al. (2021) Microstructural and mechanical properties of the plantain fiber/local clay microstructural and mechanical properties of the plantain fiber/local clay filled hybrid polystyrene composites. *Mech Adv Mater Struct* 29: 7104–7114. https://doi.org/10.1080/15376494.2021.1992692
11. Masri T, Ounis H, Sedira L, et al. (2018) Characterization of new composite material based on date palm leaflets and expanded polystyrene wastes. *Constr Build Mater* 164: 410–418. https://doi.org/10.1016/j.conbuildmat.2017.12.197
12. George A, Abdulkareem SA, Chizitere E, et al. (2022) Development and characterization of microstructural and mechanical properties of hybrid polystyrene composites filled with kaolin and expanded polyethylene powder. *Results Eng* 14: 100423. https://doi.org/10.1016/j.rineng.2022.100423
13. Taurino R, Bondioli F, Messori M (2023) Use of different kinds of waste in the construction of new polymer composites: Review. *Mater Today Sustain* 21: 100298. https://doi.org/10.1016/j.mtsust.2022.100298
14. Das O, Babu K, Shanmugam V, et al. (2022) Natural and industrial wastes for sustainable and renewable polymer composites. *Renew Sustain Energy Rev* 158: 112054. https://doi.org/10.1016/j.rser.2021.112054
15. Mathapati M, Amate K, Durga Prasad C, et al. (2022) A review on fly ash utilization. *Mater Today Proc* 50: 1535–1540. https://doi.org/10.1016/j.matpr.2021.09.106
16. Yao ZT, Ji XS, Sarker PK, et al. (2015) A comprehensive review on the applications of coal fly ash. *Earth-Science Rev* 141: 105–121. https://doi.org/10.1016/j.earscirev.2014.11.016
17. Nagrockienė D, Rutkauskas A (2019) The effect of fly ash additive on the resistance of concrete to alkali silica reaction. *Constr Build Mater* 201: 599–609. https://doi.org/10.1016/j.conbuildmat.2018.12.225
18. Li J, Li X, Liang S, et al. (2021) Preparation of water-permeable bricks derived from fly ash by autoclaving. *Constr Build Mater* 271: 121556. https://doi.org/10.1016/j.conbuildmat.2020.121556
19. Sheng G, Li Q, Zhai J (2012) Investigation on the hydration of CFBC fly ash. *Fuel* 98: 61–66. https://doi.org/10.1016/j.fuel.2012.02.008
20. Moukannaa S, Bagheri A, Benzaazoua M, et al. (2020) Elaboration of alkali activated materials using a non-calcined red clay from phosphate mines amended with fly ash or slag: A structural study. *Mater Chem Phys* 256: 123678. https://doi.org/10.1016/j.matchemphys.2020.123678
21. Nath DCD, Bandyopadhyay S, Yu A, et al. (2009) Structure-property interface correlation of fly ash-isotactic polypropylene composites. *J Mater Sci* 44: 6078–6089. https://doi.org/10.1007/s10853-009-3839-3
22. ASTM International (1999) Standard test method for water absorption, bulk density, apparent porosity, and apparent specific gravity of fired whiteware products. ASTM C373-14, 88: 1–2.
23. Zhang L, Zhou M, Meng F, et al. (2025) Recent advances in chemiresistive gas sensor for acetone detection: Focus on room temperature. *TrAC Trends Anal Chem* 187: 118213. https://doi.org/10.1016/j.trac.2025.118213

24. Bicer A, Kar F (2017) Thermal and mechanical properties of gypsum plaster mixed with expanded polystyrene and tragacanth. *Therm Sci Eng Prog* 1: 59–65. https://doi.org/10.1016/j.tsep.2017.02.008
25. Hittini W, Abu-Jdayil B, Mourad AH (2019) Development of date pit–polystyrene thermoplastic heat insulator material: Mechanical properties. *J Thermoplast Compos Mater* 2019: 697627. https://doi.org/10.1155/2019/1697627
26. Li Z, Zhang Q, Cui J, et al. (2025) Ecofriendly flame-retardant polystyrene composites: Exploiting the synergistic effects of phytic acid, polyethyleneimine, and expandable graphite. *Materials* 18: 4038. https://doi.org/10.3390/ma18184308
27. Nciri N, Shin T, Cho N (2020) Towards the use of waste expanded polystyrene as potential modifier for flexible road pavements. *Mater Today Proc* 24: 763–771. https://doi.org/10.1016/j.matpr.2020.04.384
28. Maurya AK, Gogoi R, Manik G (2021) Study of the moisture mitigation and toughening effect of fly-ash particles on sisal fiber-reinforced hybrid polypropylene composites. *J Polym Environ* 29: 2321–2336. https://doi.org/10.1007/s10924-021-02043-3
29. Ge JC, Lee ES, Kim DJ, et al. (2023) Preparation of waste PP/fly ash/waste stone powder composites and evaluation of their mechanical properties. *Materials* 16: 3687. https://doi.org/10.3390/ma16103687
30. Almusawi A, Lachat R, Atcholi KE et al. (2017) Manufacturing and characterisation of thermoplastic composite of hemp shives and recycled expanded polystyrene. *AIP Conf Proc* 1914: 170001. https://doi.org/10.1063/1.5016784
31. Adeniyi AG, Abdulkareem S, Ighalo JO, et al. (2020) Morphological and thermal properties of polystyrene composite reinforced with biochar from elephant grass (Pennisetum purpureum). *J Thermoplast Compos Mater* 35: 1532–1547. https://doi.org/10.1177/0892705720939169
32. Pramoda KP, Lim QF, Chen S (2018) Synergistic effects of fillers on recycled polystyrene composites. *Polym Bull* 75: 1185–1195. https://doi.org/10.1007/s00289-017-2085-0
33. Mumbach GD, Bolzan A, Antonio R, et al. (2020) A closed-loop process design for recycling expanded polystyrene waste by dissolution and polymerization. *Polymer* 209: 122940. https://doi.org/10.1016/j.polymer.2020.122940
34. Cunha RDS, Mumbach GD, Antonio R, et al. (2021) A comprehensive investigation of waste expanded polystyrene recycling by dissolution technique combined with nanoprecipitation. *Environ Nanotechnol Monit Manage* 16: 100470. https://doi.org/10.1016/j.enmm.2021.100470
35. Chaudhary AK, Vijayakumar RP (2020) Studies on biological degradation of polystyrene by pure fungal cultures. *Environ Dev Sustain* 22: 4495–4508. https://doi.org/10.1007/s10668-019-00394-5
36. Albunia AR, Musto P, Guerra G (2006) FTIR spectra of pure helical crystalline phases of syndiotactic polystyrene. *Polymer* 47: 234–242. https://doi.org/10.1016/j.polymer.2005.10.135
37. Iqbal A, Sattar H, Haider R, et al. (2019) Synthesis and characterization of pure phase zeolite 4A from coal fly ash. *J Clean Prod* 219: 258–267. https://doi.org/10.1016/j.jclepro.2019.02.066

38. Zhang Z, Wang H, Provis JL (2012) Quantitative study of the reactivity of fly ash in geopolymerization by FTIR. *J Sustain Cem Mater* 1: 154–166. https://doi.org/10.1080/21650373.2012.752620

AIMS Press